31st Annual International Conference of the IEEE EMBS
Minneapolis, Minnesota, USA, September 2-6, 2009

Tissue vibration pulsatility for arterial bleeding detection using Doppler ultrasound

Zhiyong Xie, Eung-Hun Kim and Yongmin Kim
Department of Bioengineering, University of Washington, Seattle, WA 98195, USA

Abstract—**Trauma is the number one cause of death among Americans between 1 and 44 years old, and exsanguination due to internal bleeding resulting from arterial injuries is a major factor in trauma deaths. We have evaluated the feasibility of using tissue vibration pulsatility in arterial bleeding detection. Eight femoral arteries from four juvenile pigs were punctured transcutaneously with a 6 or 9-French catheter. Also, 11 silicone vessels wrapped with turkey breast were placed in a pulsatile flow phantom and penetrated with an 18-gauge needle. The tissue vibration pulsatility was derived as a ratio of the maximum spectral energy from 200 to 2500 Hz of tissue vibration in systole over a baseline value in diastole. Then, the tissue vibration pulsatility index (TVPI) was defined as the maximum tissue vibration pulsatility value for each experimental condition. Both *in vitro* and *in vivo* results showed that the TVPI from injured vessels is significantly higher ($p<0.005$) than that of intact vessels. In addition, we constructed the 2D map of tissue vibration pulsatility during *in vitro* studies and found that it could be used for spatial localization of the puncture site. Our preliminary results indicate that the tissue vibration pulsatility may be useful for detecting arterial bleeding and localizing the bleeding site.**

Keywords—**Perivascular tissue vibration, tissue vibration pulsatility, Doppler ultrasound, arterial bleeding detection.**

I. Introduction

Trauma is the number one cause of death among Americans between 1 and 44 years old, and the trauma death rate from all causes combined has increased since 1992 [1]. Exsanguination due to internal bleeding resulting from arterial injuries is a major factor in trauma deaths. Therefore, rapid and effective diagnosis of arterial bleeding is essential for providing timely treatment and reducing the mortality.

Diagnostic peritoneal lavage (DPL), X-ray CT and ultrasonography have been used for prompt diagnosis of arterial bleeding. DPL is cost-effective and highly sensitive, but it is invasive and lacks specificity [2]. While X-ray CT is sensitive and specific [3], it is costly and time-consuming. Ultrasound is attractive due to its portability, low cost and noninvasiveness. However, conventional ultrasound suffers from insufficient sensitivity. To improve the sensitivity, various ultrasound imaging techniques have been studied. Contrast-enhanced sonography improves sensitivity [4], but the contrast agent used may cause adverse bioeffects including microvascular leakage [5]. Doppler ultrasound has been used in qualitatively detecting bleeding based on the presence of characteristic features from blood flow turbulence [6], but it is time-consuming and requires well-trained sonographers. Quantitative flow parameters from spectral Doppler, such as resistance index, have been evaluated for bleeding detection, but it is operator-dependent [7, 8, 9].

Perivascular tissue vibration is another indicator for bleeding [10]. Audible bruits and palpable thrills caused by tissue vibration have been considered as a hard sign of arterial injuries during examinations of trauma patients [11], but this approach is not sensitive since only vibrations with sufficient power can reach the skin surface. Also, tissue vibration appears as perivascular artifacts on color Doppler images and a bidirectional pattern in spectral Doppler waveforms [12]. However, these vibration signatures are qualitative and hard to interpret [10]. More recent studies introduced several signal processing algorithms to estimate vibration characteristics using Doppler ultrasound [10, 13]. They reported that bleeding detection methods based on tissue vibration could be more reliable, more sensitive and less operator-dependent than conventional Doppler ultrasound. To assess tissue vibration more quantitatively for bleeding detection, we have developed a new metric, i.e., tissue vibration pulsatility, based on the spectral energy characteristics of tissue vibration velocity obtained from Doppler ultrasound. We have evaluated the feasibility of using tissue vibration pulsatility in detecting penetrating arterial injuries and locating the bleeding site.

II. Methods and Materials

A. Tissue vibration pulsatility

Figure 1 shows the flow chart of tissue vibration pulsatility calculation process at a specific depth in the Doppler range gate along a scanline. The steps involved are: 1) estimate the instantaneous tissue velocity $v_i(t)$ using a modified autocorrelation method,

$$v_i(t)=\frac{c\times f_{PRF}}{4\pi f_0}\arg<\sum_{j=i-2}^{i+2}(y(j,m)\times y^*(j,m-1))> \quad (1)$$

where c is the velocity of sound in blood, f_{PRF} is the pulse repetition frequency, f_0 is the transducer center frequency, $y(j,m-1)$ and $y(j,m)$ are the complex signals received from $(m-1)^{th}$ and m^{th} pulse transmission at j^{th} depth, respectively. Phase shift is averaged with five successive depth points (i-2 to i+2) to improve the signal-to-noise ratio; 2) compute the time-varying spectral energy of instantaneous tissue velocity by 256-point zero-padded short-time Fourier transform using a 20-ms long and 50%-overlapped time window; 3) sum the

This work was supported in part by a grant from National Institutes of Health (Grant No. NIH 5-R21-GM076086).

spectral energy of instantaneous tissue velocity in the 200~2500 Hz frequency band; 4) compute the tissue vibration pulsatility as the ratio of the maximum spectral energy of tissue vibration in systole over a baseline value in diastole during one cardiac cycle as shown in the right side of Fig. 1; 5) repeat step 4 for every cardiac cycle, typically 5 to 15 cycles, and 6) the tissue vibration pulsatility for a specific depth is the median of measured tissue vibration pulsatility values.

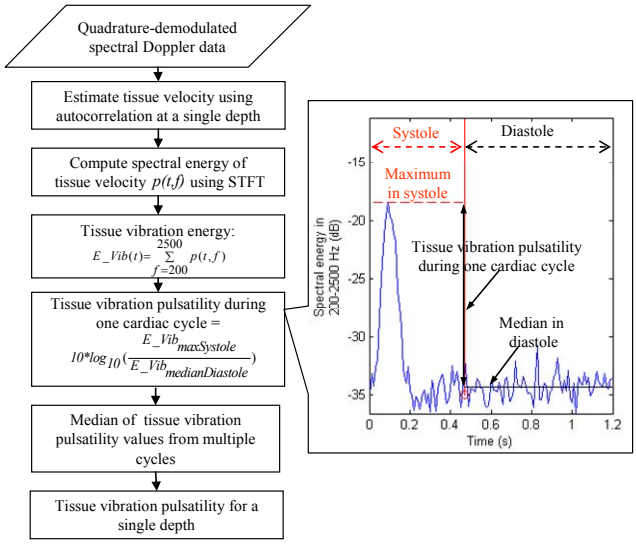

Figure 1. Flow chart of tissue vibration pulsatility calculation steps for a single depth.

By repeating the tissue vibration pulsatility calculation process for all depths in a single scanline and repeating this for all acquired scanlines, a 2D map of tissue vibration pulsatility values for each experimental condition could be generated. The tissue vibration pulsatility index (TVPI) is defined as the maximum tissue vibration pulsatility value in the 2D map to capture the strongest tissue vibration pulsatility in the control or injury case for each experimental condition.

B. *Experimental setup*

To provide a relatively controlled environment, a pulsatile flow phantom was used for the *in vitro* study. The phantom had been developed previously [14], but we embedded a vessel (a 40-cm long silicone tube (Silcon®, New Age Industries, Southampton, PA) with the inner diameter of 6.35 mm and the outer diameter of 7.95 mm) in the turkey breast instead of the agarose gel. Figure 2 shows a schematic diagram of the phantom. Blood-mimicking fluid composed of 5 µm Orgasol™ (2001USNAT1 Orgasol, ELF Autochem, Paris, France) particles and water was continuously delivered through a 'test vessel' via a solenoid actuated metering pump (E-plus, Pulsafeeder, Punta Gorda, FL). Turkey breast was wrapped around the vessel to try to mimic an *in vivo* situation. The air volume in the damping column was used to control the systolic pressure while the valve in the outlet was used to adjust the diastolic pressure. A pressure gauge (Ultraview SL, Spacelabs Healthcare, Issaquah, WA) was used to monitor the vessel pressure. The pulsatile flow was produced by the phantom with the peak systolic flow velocity of 31.1 to 113.0 cm/s, the pulse rate of 45-138 beats/min and the peak systolic pressure of 90 to 250 mmHg. To model penetrating arterial injuries, 11 vessels were punctured through turkey breast with an 18-gauge needle. Data were acquired before and immediately after puncture at various locations along the vessel.

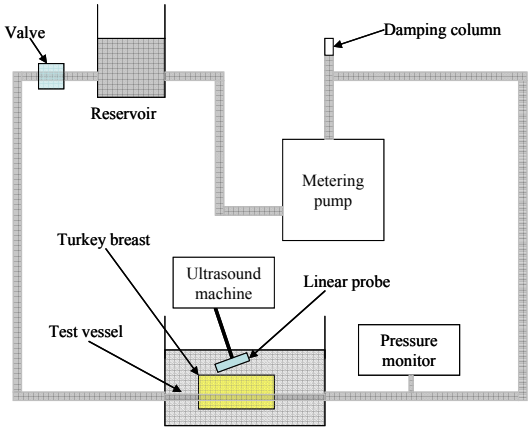

Figure 2. Schematic diagram of the *in vitro* experimental setup.

For the *in vivo* study, four anesthetized juvenile pigs were used, following the protocol approved by the University of Washington Institutional Animal Care and Use Committee. Both femoral arteries (diameter of about 0.5 cm) from each pig were punctured using a 6 or 9-French catheter to simulate penetrating arterial injuries. Data were acquired before and immediately after the injury.

C. *Data acquisition*

For both *in vitro* and *in vivo* studies, a clinical ultrasound machine (Hi Vision 5500, Hitachi Medical Systems America, Twinsburg, OH) was used to acquire raw ultrasound data with a 6 to 13-MHz linear probe. The baseband, quadrature-demodulated data were collected from a 15-mm range gate in spectral Doppler mode (PRF of 2 to 12 kHz).

III. Results and Discussion

A. *TVPI from control and injury cases*

Figure 3 shows the TVPI of intact and punctured vessels from the *in vitro* study. The TVPI from punctured vessels (23.67 ± 10.95 dB) is higher than that from non-punctured vessels (5.66 ± 3.42 dB). A p-value of 0.0001 was obtained via a two-sample one-sided t-test between the TVPIs from punctured and non-punctured vessels, which indicates that the difference between two sets is significant. The pulsatile phantom in our *in vitro* study provides a reproducible environment and allows us to control various flow dynamic parameters.

Figure 4 shows the TVPI between intact and injured arteries *in vivo*. The results are similar to the *in vitro* study. The TVPI from the perivascular tissues of injured arteries (14.73 ± 8.60 dB) is significantly higher (p=0.0047) than that of non-injured arteries (4.00 ± 1.80 dB). The pig femoral artery bleeding model used in our *in vivo* study represents a more realistic scenario of human injuries since the

cardiovascular system of a pig is similar to that of human [8]. Thus, this result in pigs suggests that tissue vibration pulsatility may be applicable to detecting arterial bleeding in humans.

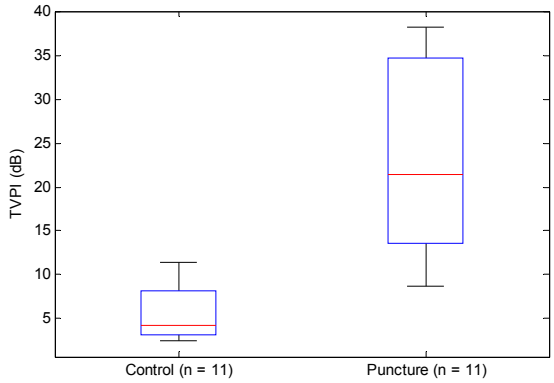

Figure 3. TVPI of intact and punctured vessels *in vitro*.

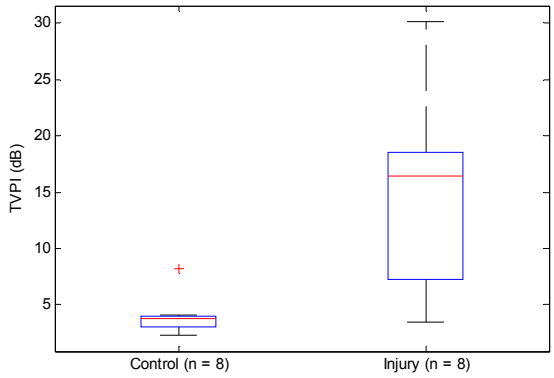

Figure 4. TVPI of control and injury vessels *in vivo*.

The TVPI in the punctured vessels from the *in vitro* study is significantly higher (p=0.03) than that in the injured arteries *in vivo*. This difference might be caused by several reasons. One is that *in vitro* environment is more stable and free from additional complications. Bleeding *in vitro* is not affected by clotting process, thus the tissue vibration pulsatility does not drop as much compared to bleeding *in vivo*. Second, the *in vitro* vessel pressure was higher than that in *in vivo* cases. A higher pressure would increase the leakage velocity, and the vibration pulsatility would become stronger with a higher peak systolic velocity in the jet. No significant difference (p=0.19) was found between the TVPI in *in vitro* intact vessels and that in *in vivo* intact arteries.

TVPI variance from *in vitro* and *in vivo* puncture cases is much higher than that from the corresponding control cases as shown in Figs. 3 and 4. There are several reasons for this large variance. First, the shape of bleeding jet (e.g., curvature, direction and length) in turkey breast or femoral arteries in pigs might have varied in different experiments even though the needle or catheter used for puncture had the same diameter. We had investigated agar phantoms with a pre-built puncture of fixed shape, where the variance was much smaller. Second, in our *in vitro* experiments, we did not have a very good control of pressure after puncture and could not minimize the intra-experiment pressure change. The peak systolic pressure change would have affected the leakage jet velocity and vibration in the soft tissue. Better control of the pressure would help decrease the TVPI variance. Third, compared with control cases, the spatial distribution of vibrations in puncture cases is more dispersed along the pulsatile flow direction since the tissue vibration strength falls off sharply with the increasing distance from the vibration source.

B. 2D map of tissue vibration pulsatility

We can generate a 2D map of the tissue vibration pulsatility, which could be helpful in localizing the bleeding site. Figure 5 shows the color Doppler image of a punctured vessel during an *in vitro* experiment. Pulsatile flow is pumped through the vessel from right to left with the peak systolic velocity of 88.2 cm/s and the pulse rate of 70 beats/min. As shown in Fig. 5, bleeding is shown as the jet with a red-blue checkered pattern extending from the puncture site in the vessel, which suggests turbulent flow caused by the injury. After puncture, spectral Doppler data were acquired along 12 scanlines that are parallel with the bleeding jet: D6, D5, D4, D3, D2, D1 and D0 are distal to the puncture site along the pulsatile flow direction, while U0, U1, U2, U3, and U4 are proximal to the puncture site. The overall image depth is 30 mm from the probe as shown in Fig. 5.

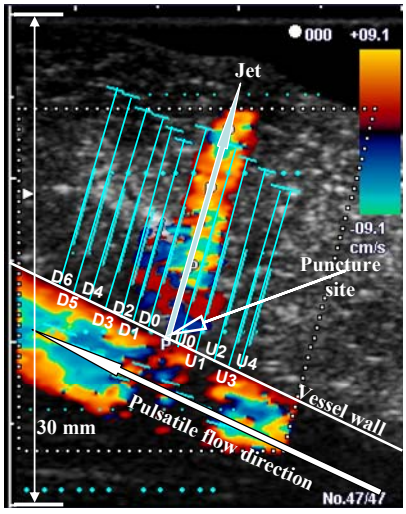

Figure 5. Color Doppler image of a punctured vessel.

Figure 6 shows a 2D map of tissue vibration pulsatility in perivascular tissue surrounding the puncture site. The tissue vibration pulsatility is expected to be higher near the vibration source, so the locations of high tissue vibration pulsatility are likely to be the vibration sources as shown in Fig. 6. Our preliminary result indicates that vibration sources are located at the downstream of the bleeding jet where turbulent eddies are formed. We can localize the puncture site by identifying vibration sources due to their close spatial relationship. However, more studies are needed on how to accurately determine the exact puncture site based on vibration sources.

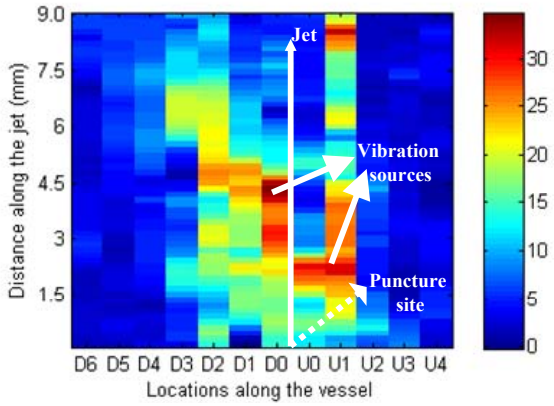

Figure 6. A 2D map of tissue vibration pulsatility surrounding the puncture site.

The bleeding site localization method with a 2D map of tissue vibration pulsatility offers a potential advantage over the ones based on color Doppler. In color Doppler acquisition, the ultrasound beam sweeps across an area of interest in order to acquire data from multiple scanlines, thus there is a significant time interval between forming a scanline in one frame and forming the same scanline in the next frame. For a color Doppler system with the scanline number of 192 and the frame rate of 7.9~25.57 [15], the time interval would be 38.9~125.9 ms. Some or entire part of tissue vibration, of which duration typically lasts 10 to 150 ms, could be missed in localization methods based on color Doppler due to the time interval [16]. In spectral Doppler acquisition, data are acquired along a single scanline with much finer temporal resolution by sacrificing the field of view. By reconstructing a 2D map of tissue vibration pulsatility from multiple scanlines acquired from spectral Doppler, we could expand the field of view without missing vibrations. One limitation of our localization method is that scanlines for reconstructing a 2D map of tissue vibration pulsatility are acquired line-by-line at different times. It remains to be seen whether respiration and cardiac motion would affect the effectiveness of our localization method and whether motion effects in localization can be reduced by using gating techniques.

IV. Conclusion

Our preliminary results from *in vitro* and *in vivo* studies show that the tissue vibration pulsatility is capable of detecting the tissue vibrations that occur at the penetrating vascular injuries. Also, a 2D map of tissue vibration pulsatility may be useful in localizing the bleeding site in arterial injuries. Tissue vibration pulsatility could complement color and spectral Doppler for arterial bleeding detection with additional information, and potentially provide guidance for future intraoperative hemostasis procedures by localizing and monitoring the active bleeding site.

Acknowledgment

The authors gratefully acknowledge the contributions of Dr Siddhartha Sikdar, Nikita Imennov, Xinliang Zheng, Dr Shahram Vaezy, Ting Xia, Sepideh Zolfaghari and Hamid Hosseini for assistance with *in vivo* and *in vitro* studies.

References

[1] H. C. Kung, D. L. Hoyert, J. Xu, and S. L. Murphy, "Deaths: final data for 2005," *Natl Vital Stat Rep*, vol. 56(10), pp. 7–9, 2008. Available at: www.cdc.gov/nchs/data/nvsr/nvsr56/nvsr56_10.pdf. Accessed April 10, 2009.

[2] P. J. Bode, R. A. Niezen, A. B. van Vugt and J. Schipper, "Abdominal ultrasound as a reliable indicator for conclusive laparotomy in blunt abdominal trauma," *J Trauma.*, vol. 34, pp. 27-31, 1993.

[3] P. D. Peng, D. A. Spain, M Tataria, J. C. Hellinger, G. D. Rubin, and S. I. Brundage, "CT angiography effectively evaluates extremity vascular trauma," *The American Surgeon*, vol. 74, pp. 103-107, 2008.

[4] W. Luo, V. Zderic, S. Carter, L. Crum, S. Vaezy, "Detection of bleeding in injured femoral arteries with contrast-enchanced sonography," *J Ultrasound Med.*, vol. 25, pp. 1169-1177, 2006.

[5] D. L. Miller, M. A. Averkiou, A. A. Brayman, E. C. Everbach, C. K. Holland, J. H. Wible and J. Wu, "Bioeffects Considerations for Diagnostic Ultrasound Contrast Agents," *J Ultrasound Med.*, vol. 27, pp. 611-632, 2008.

[6] D. Gaitini, N. B. Razi, E. Ghersin, A. Ofer, M. Soudack, "Sonographic evaluation of vascular injuries," *J Ultrasound Med.*, vol. 27, pp. 95-107, 2008.

[7] A. Anand, J. Petruzzello, S. Yin, B. Dunmire, J. Kucewicz and S. Vaezy, "Noninvasive bleeding detection and localization using three dimensional Doppler ultrasound," *IEEE Ultrasonics Symposium*, pp. 1297-1300, 2007.

[8] W. Luo, V. Zderic, F. A. Mann, and S. Vaezy, "Color and pulsed Doppler sonography for arterial bleeding detection," *J Ultrasound Med.*, vol. 26, pp. 1169-1177, 2007.

[9] D. Yang, D. Zhang, X. Guo, X. Gong and X. Fei, "A multi-dimensional approach for describing internal bleeding in an artery: implications for Doppler ultrasound guiding HIFU hemostasis," *Phys. Med. Biol*, vol. 53, pp: 4983–4994, 2008.

[10] S. Sikdar, K. W. Beach, S. Vaezy, and Y. Kim, "Ultrasonic interrogation of tissue vibration in arterial and organ injuries: preliminary *in vivo* results," *Ultrasound Med. Biol.,* vol. 32, pp. 1203-1214, 2006.

[11] J. T. Anderson, and W. F. Blaisdell, Diagnosis of Vascular Trauma. In: Rich NM, ed. Vascular Trauma. Philadelphia, PA: Saunders, pp: 113-124, 2004.

[12] W. D. Middleton, S. Erikson, and G. L. Melson, "Perivascular color artifact: Pathological significance and appearance on color Doppler images," *Radiology*, vol. 171, pp. 647– 652, 1989.

[13] M. I. Plett and K. W. Beach, "Ultrasonic vibration detection with wavelets: preliminary results," *Ultrasound Med. Biol.,* vol. 31, pp. 367-375, 2005.

[14] R. Greaby, V. Zderic, and S. Vaezy, "Pulsatile flow phantom for ultrasound image-guided HIFU treatment of vascular injuries," *Ultrasound Med. Biol.*, vol. 33, pp. 1269-1276, 2007.

[15] V. Shamdasani, R. Managuli, S. Sikdar, and Y. Kim, "Ultrasound color-flow imaging on a programmable system," *IEEE Trans. Inf. Technol. Biomed.*, vol. 8, pp. 191-199, 2004.

[16] S. Sikdar, K. W. Beach, S. Vaezy, and Y. Kim, "Ultrasonic technique for imaging tissue vibrations: preliminary results," *Ultrasound Med. Biol.,* vol. 31, pp. 221-232, 2005.